

Article

Preparation of ZrO₂/Graphene Oxide/TiO₂ Composite Photocatalyst and Its Studies on Decomposition of Organic Matter

Yu-Hsun Nien ^{*}, Jih-Fong Chen, Cai-Yin Fang and Ming-Sheng Liu

Department of Chemical and Materials Engineering, National Yunlin University of Science and Technology, Douliou 64002, Taiwan; m10515034@yuntech.edu.tw (J.-F.C.); B10815104@yuntech.edu.tw (C.-Y.F.); m11015046@yuntech.edu.tw (M.-S.L.)

* Correspondence: nienyh@yuntech.edu.tw

Abstract: Water polluted by organic dyes is a serious environmental problem. In response to this, the aim of this research is to degrade dye wastewater using a modified photocatalyst. Since sunlight only has less than 5% UV energy, for a general photocatalyst, using sunlight for excitation to decompose organic pollutants is not an effective way. Therefore, we manufactured the modified photocatalyst by zirconium dioxide, graphene oxide, and titanium dioxide. This was to better improve the photo-degradation efficiency for the degradation of organic pollutants. The modified photocatalyst was analyzed by X-ray diffractometer (XRD), Fourier-transform infrared spectroscopy (FT-IR), Raman spectroscopy (Raman), Scanning Electron Microscope (SEM), and Energy-dispersive X-ray spectroscopy (EDS). The results demonstrated that the modified photocatalyst can be activated by the absorption of visible light. Additionally, the band gap of the modified photocatalyst would decrease. The photodegradation percentage of the modified photocatalyst under visible light (Philips TL-D 8W/865 fluorescent tube) for 4 h reached up to 49.92%. At the third test after ultrasonic washing for the cyclic test, the photodegradation percentage of the modified photocatalyst could still maintain at 47.71%. This indicates that the modified photocatalyst has good stability and reusability, and so this can be reused in this regard.

Keywords: ZrO₂; TiO₂; photocatalyst



Citation: Nien, Y.-H.; Chen, J.-F.; Fang, C.-Y.; Liu, M.-S. Preparation of ZrO₂/Graphene Oxide/TiO₂ Composite Photocatalyst and Its Studies on Decomposition of Organic Matter. *J. Compos. Sci.* **2022**, *6*, 9. <https://doi.org/10.3390/jcs6010009>

Academic Editor: Jian-Zhang Chen

Received: 29 November 2021

Accepted: 24 December 2021

Published: 29 December 2021

Publisher's Note: MDPI stays neutral with regard to jurisdictional claims in published maps and institutional affiliations.



Copyright: © 2021 by the authors. Licensee MDPI, Basel, Switzerland. This article is an open access article distributed under the terms and conditions of the Creative Commons Attribution (CC BY) license (<https://creativecommons.org/licenses/by/4.0/>).

1. Introduction

With the rapid development of industry, it is inevitable for environmental pollution to occur. Pollution mainly includes discharged wastewater, and dye wastewater is the bulk of it. Therefore, the problem of dye wastewater must be solved. To better deal with this problem, photocatalysis is a preferred method. Titanium dioxide is considered an attractive material because it has the following advantages of low-cost, non-toxicity, no secondary pollution, and chemical stability. However, TiO₂ still remains limited during this practice. For example, it takes higher energy, when compared with the band gap of TiO₂ (3.2 eV), to generate electrons by means of exciting titanium dioxide. In other words, a high-energy beam, such as ultraviolet light, can be used for photoexcitation to rather achieve the effect of decomposing organic matter. However, in solar radiation, there is only 3–5% of ultraviolet light, and this is insufficient. In addition, the rapid combination of excited electron–hole pairs also loses their original redox ability, thereby causing it to decompose organic matter. Titanium dioxide with a wide band-gap metal oxide is currently the most studied photocatalytic material. Through the doping of other metals (platinum, gold, silver, copper, and zinc), it is believed that the doping of platinum can possibly increase the separation of electrons and holes. Platinum deposition on the surface is able to enhance the separation of charges in photocatalysis, thereby increasing the lifetime of the electron–hole pair [1]. When carbon is added to Ti(OH)₂ in a 10-bar pressure reactor

for hydrolysis, a carbon-modified TiO₂ photocatalyst can be formed. Under the irradiation of an ultraviolet lamp and artificial sunlight, the catalyst activity of the carbon-containing titanium dioxide photocatalyst is higher than that of pure titanium dioxide. It is mainly due to the good electronic conduction of carbon atoms [2]. In order to better improve the photodegradation of traditional TiO₂, in this study, commercial titanium dioxide (P25) was used for modification by zirconium dioxide (ZrO₂) and graphene oxide (GO). The P25/ZrO₂/GO composite photocatalyst can possibly reduce the recombination of electrons and holes and increase the reaction area and the photoactivity under visible light.

2. Experimental

2.1. Material

Ethanol (purity 95%) was purchased from Taiwan Sugar Co., Ltd. as solvent. Acetone, deionized water, and sodium nitrate (purity $\geq 99.5\%$) were purchased from Sigma-Aldrich. Graphite (purity 99.99%) was purchased from Alfa Aesar. Sulfuric acid (purity $\geq 95\text{--}98\%$) was purchased from Nihon Shiyaku Industries, Ltd., Japan. Hydrochloric acid (purity 37%) was purchased from Nihon Shiyaku Industries, Ltd., Japan. Potassium permanganate (purity $\geq 99\%$) was obtained from Merck. Hydrogen peroxide (purity 35%) was purchased from Choneye Pure Chemical. Methylene Blue was acquired from Fluka-Sigma-Aldrich. Acetic acid (purity 99.81%) was purchased from Choneye Pure Chemical. Zirconium oxychloride (purity 99%) was purchased from Artikel. Citric acid was purchased from Choneye pure chemical. Titanium Dioxide (abbreviation P25), anatase 80%/Rutile 20% were purchased from UniRegion Bio-Tech.

2.2. Experimental Methods

2.2.1. Preparation of Graphene Oxide

A total of 3 g of graphite and 3 g of sodium nitrate (NaNO₃) were put into a 1L glass beaker. After this, 138 mL of sulfuric acid was added and shaken with ultrasound for 5 min. It was then stirred in an ice bath at 0–4 °C for 10 min. During the process of stirring, 9 g of potassium permanganate was slowly added first, and then it was mixed and stirred for 24 h. The solution was kept in a water bath at 98 °C, and 150 mL of deionized water was added to neutralize the solution. Additionally, 350 mL of deionized water (by weight) was added. Finally, 30 mL of hydrogen peroxide was slowly added and stirred for 30 min to stop the oxidation. The precipitate was graphene oxide. The graphene oxide was washed with 1 L acid solution with a volume ratio of 1:10 (HCl:H₂O). Finally, the graphene oxide precipitate was washed with deionized water until pH = 7 (neutral). After removing moisture with a freeze dryer, graphene oxide powder was obtained.

2.2.2. Preparation of P25/ZrO₂ Powder

A total of 3 g of P25 was added into 20 mL of 50 wt% acetic acid and mixed by ultrasonic shaking for 10 min. Various amounts (96 mg, 192 mg, and 480 mg) of ZrOCl₂·8H₂O and the same amount of chelating agent C₆H₈O₇·H₂O were added into the P25/acetic acid solution by ultrasonic shaking for 10 min. The above solution was heated at 100 °C until it became dry. Then, the residue was put into a high temperature furnace, and it was kept at 450 °C and calcinated for 2 h. Finally, P25/ZrO₂ powder was obtained.

2.2.3. Preparation of P25/ZrO₂/GO Powder

In total, 1 g of P25/ZrO₂ powder was added into 20 mL of 40 wt% ethanol with ultrasonic shaking for 10 min. Based on 1 g of P25/ZrO₂ powder, the graphene oxide with various percentages of 0.5 wt%, 1 wt%, and 2 wt% was added into the P25/ZrO₂ solution with ultrasonic shaking for 1 h. The above solution was heated at 80 °C until it became dry. P25/ZrO₂/GO powder was obtained.

2.2.4. Electro spray of P25/ZrO₂/GO Powder

In total, 0.5 g of P25/ZrO₂/GO powder was added into 20 mL of 40 wt% ethanol with ultrasonic shaking for 10 min. A total of 10 mL of the above solution was put into a syringe. It was set up on the electro spray equipment. Aluminum foil was used as a collector. The fixed voltage was 17 kV, and the distance between the needle point and the collector was 10 cm. In addition, the fixed roller speed was 200 rpm, and the flow rate was 0.350 mL/min. Immediately after the electro spray was complete, the aluminum foil containing electro spray powder was put into an oven at 60 °C for 2 h. The P25/ZrO₂/GO powder was obtained.

Table 1 is all the material needed for preparation.

Table 1. Materials needed for preparation.

Photocatalyst	Symbol
Commercial photo catalyst P25	P25
P25 with 96 mg ZrOCl ₂ · 8H ₂ O	PZ96
P25 with 192 mg ZrOCl ₂ · 8H ₂ O	PZ192
P25 with 480 mg ZrOCl ₂ · 8H ₂ O	PZ480
P25 with 192 mg ZrOCl ₂ · 8H ₂ O and 0.5% GO	PZG0.5
P25 with 192 mg ZrOCl ₂ · 8H ₂ O and 1% GO	PZG1
P25 with 192 mg ZrOCl ₂ · 8H ₂ O and 2% GO	PZG2
P25 with 192 mg ZrOCl ₂ · 8H ₂ O and 0.5% GO by electro spray	PZG0.5 ESI
P25 with 192 mg ZrOCl ₂ · 8H ₂ O and 1% GO by electro spray	PZG1 ESI
P25 with 192 mg ZrOCl ₂ · 8H ₂ O and 2% GO by electro spray	PZG2 ESI

Those materials were characterized by X-ray diffractometer (XRD) (Rigaku, Mini-FlexII, Tokyo, Japan), Fourier-transform infrared spectroscopy (FTIR) (PerkinElmer, Spectrum One, and Autoimagic System, Waltham, MA, USA), UV-Vis spectrometer (lambda 850, PerkinElmer, Waltham, MA, USA), and Raman spectroscopy (Raman) (RMS-iHR550, HORIBA, Montpellier, France). Particle sizes were tested by Dynamic Light Scattering (DLS 90 Plus, Brookhaven Instruments Corporation, Holtsville, NY, USA).

Methylene Blue (MB) was used as an organic dye. We prepared methylene blue solutions with different concentrations and used a UV-Vis spectrometer to measure absorbance to calculate the calibration curve for the methylene blue solution. The methylene blue solution was decomposed by the various photocatalysts, which were PZ, PZG, and PZG ESI.

$$\text{Photodegradation rate} = [(\text{absorbance in dark} - \text{absorbance under light}) / \text{original absorbance}] \times 100\%$$

Original absorbance is the absorbance of methylene blue solution without adding photocatalyst powder. Absorbance under light is the absorbance of methylene blue solution added with photocatalyst powder under light.

Absorbance in dark is the absorbance of methylene blue solution with photocatalyst powder added in dark.

The photodegradation of methylene blue was tested beside a Philips TL-D 8W/865 fluorescent tube for 4 h.

3. Results and Discussion

3.1. Analysis of Graphene Oxide (GO)

3.1.1. XRD Analysis of Graphene Oxide (GO)

When graphite is oxidized with strong oxidants, graphene oxide can be obtained. In this study, graphene oxide maintains the hexagonal lattice structure. There are many oxygen-containing functional groups on the surface of carbon, e.g., carboxylic, hydroxyl, and epoxy groups. These oxygen-containing functional groups open up the distance between carbon and carbon layers, which reduce the 2θ angle [3]. Graphene oxide (GO), as

shown in Figure 1, has a distinct characteristic peak at $2\theta = 10.9^\circ$ [4], and a broad diffraction peak appears at $2\theta = 24.9^\circ$. This indicates a typical graphene oxide characteristic peak.

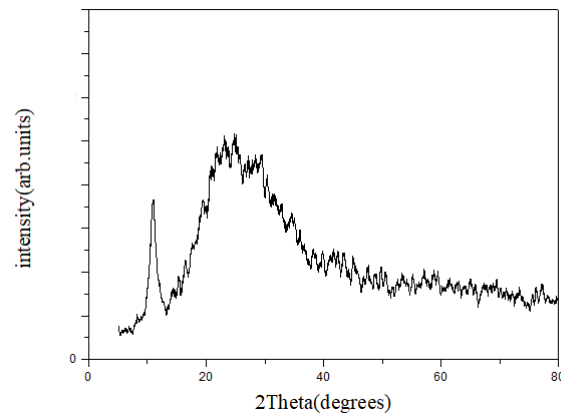


Figure 1. X-ray diffractometer (XRD) of graphene oxide.

3.1.2. FT-IR Analysis of Graphene Oxide (GO)

The FT-IR of graphene oxide (GO) is shown in Figure 2. The peak at 3410 cm^{-1} is the stretching vibration of the -OH group. The peak at 1718 cm^{-1} is the stretching vibration of the carboxyl group. The peak at 1614 cm^{-1} is the C=C group plane stretching vibration. A total of 1384 cm^{-1} was OH deformation, 1235 cm^{-1} was the stretching vibration of C-OH, and 1057 cm^{-1} was the stretching vibration of CO. This part of the results is consistent with that documented in the literature [5].

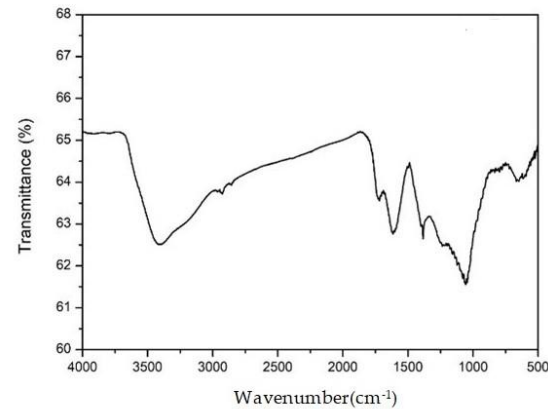


Figure 2. Fourier-transform infrared spectroscopy (FT-IR) of graphene oxide.

3.1.3. Raman Analysis of Graphene Oxide (GO)

In Figure 3, graphene oxide (GO) has two strong characteristic peaks, which are the D band signal of 1357.5 cm^{-1} and the G band signal of 1595.9 cm^{-1} . The D band signal is the vibration of the edge of the carbon crystalline state. Clearly, when the D band becomes strong, the surface tends to defect; the G band signal is caused by the plane vibration of the graphene oxide sp^2 carbon atoms. The graphene oxide we prepared had an I_D/I_G of 0.83. This part of the results derived from this study is similar to that of the previous literature [6] because when I_D/I_G is 0.82, I_D/I_G is an index for judging the disorder in related defects, such as vacancies, grain boundaries, and amorphous carbon in graphene oxide.

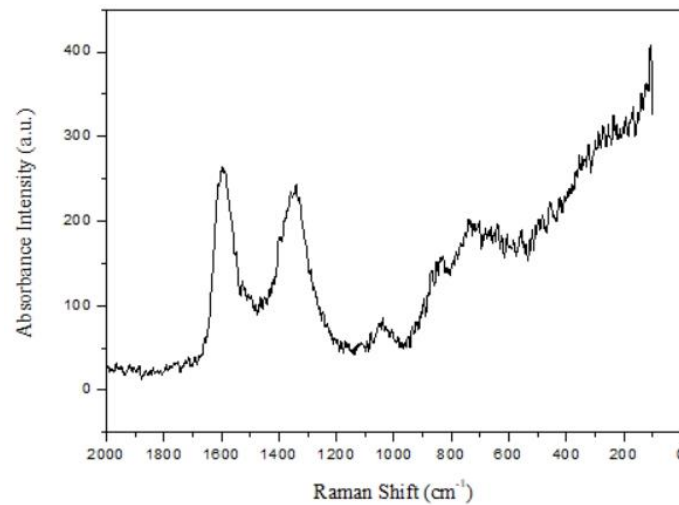


Figure 3. Raman spectroscopy (Raman) of graphene oxide.

3.2. Analysis of P25/ZrO₂

3.2.1. XRD Analysis of P25/ZrO₂

When compared with Joint Committee on Powder Diffraction Standard (JCPDS) standard chart No.21-1276, the diffraction peaks of titanium dioxide anatase were at $2\theta = 25.52^\circ, 37.76^\circ, 48.06^\circ, 54.08^\circ, 55.06^\circ, 63.02^\circ, 69.24^\circ, 70.40^\circ,$ and 75.46° as shown in Figure 4. The diffraction peaks of titanium dioxide rutile were at $2\theta = 27.3^\circ, 36.0^\circ, 39.10^\circ, 41.2^\circ, 44.0^\circ,$ and 56.6° . However, the P25/ZrO₂ prepared in this study showed a higher anatase content. When compared with JCPDS standard chart No.37-1484, the characteristic peaks of zirconium dioxide monoclinic crystals were at $2\theta = 28.2^\circ$ and 31.4° . Besides, when compared with JCPDS standard chart No.80-0965, the characteristic peaks of the cubic phase of zirconium dioxide were at $2\theta = 35.2^\circ, 50.6^\circ,$ and 60.2° . The content of ZrO₂ in P25/ZrO₂ was scarce, and this made the peaks opaque. This part of the results lends support to that of the previous literature [7].

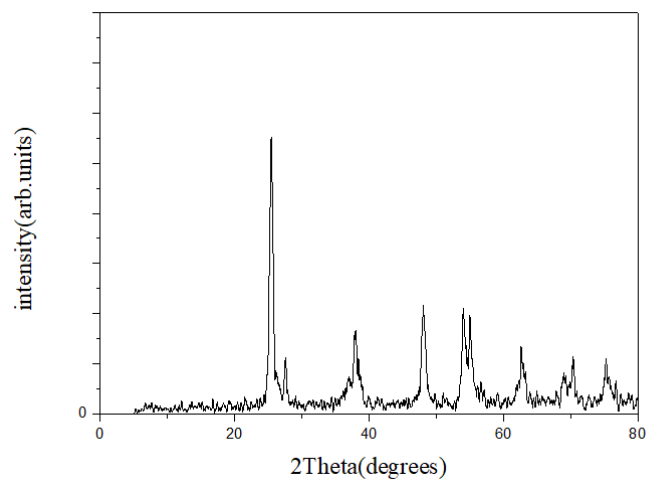


Figure 4. XRD of P25/ZrO₂.

3.2.2. UV-Vis Spectrum of Various Ratios of P25/ZrO₂

Generally, the wavelength from 250 nm to 400 nm is in the ultraviolet light region, and 400–780 nm is the visible light region. From Figure 5, after adding zirconium dioxide, the initial absorption wavelength shows a slight red shift. The more amount added, the more the red shifted.

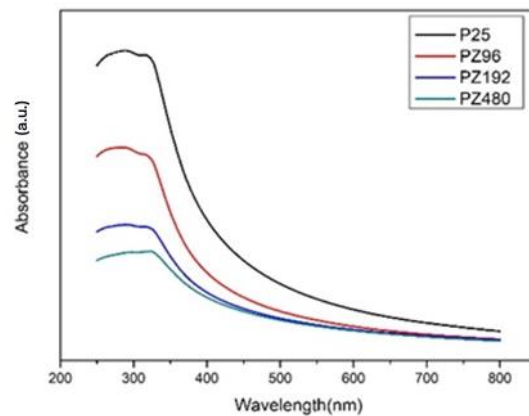


Figure 5. UV-Vis of various ratios of P25/ZrO₂.

3.2.3. Energy Gap Analysis of Various Ratios of P25/ZrO₂

Generally, the energy gap of TiO₂ photocatalyst is about 3.2 eV. From Figure 6, the energy gap of P25 is about 3.29 eV based on Kubelka-Munk coordinates. After adding zirconium dioxide, the energy gap tended to decrease.

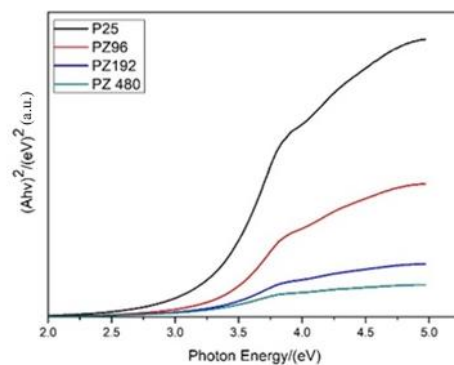


Figure 6. Energy gap analysis of various ratios of P25/ZrO₂.

3.2.4. EDS Analysis of Various Ratios of P25/ZrO₂

The P25/ZrO₂ was analyzed using EDS.

According to the results of the EDS analysis, the presence of Zr could be detected in the composite material as shown in Tables 2–4 and Figures 7–9.

Table 2. PZ96 Photocatalyst element analysis.

Element	Weight (%)	Atom. (%)	Error (%)
Oxygen(O)	50.53	73.57	16.0
Titanium(Ti)	47.10	22.91	3.4
Zirconium(Zr)	0.63	0.16	0.1

Table 3. PZ192 Photocatalyst element analysis.

Element	Weight (%)	Atom. (%)	Error (%)
Oxygen(O)	46.19	72.20	17.7
Titanium(Ti)	52.58	27.46	3.5
Zirconium(Zr)	1.22	0.34	0.2

Table 4. PZ480 Photocatalyst element analysis.

Element	Weight (%)	Atom. (%)	Error (%)
Oxygen(O)	45.92	71.10	18.4
Titanium(Ti)	50.20	25.97	3.4
Zirconium(Zr)	2.83	0.77	0.4

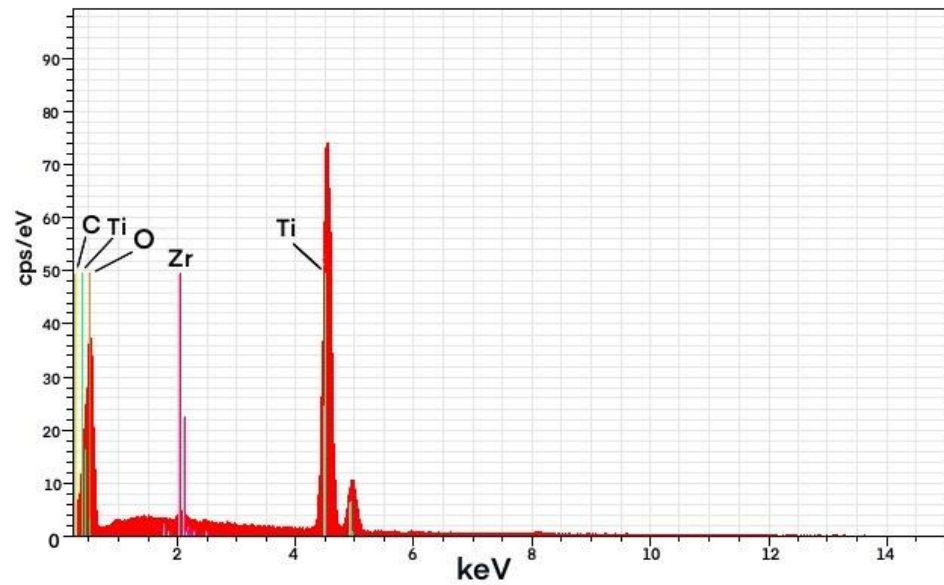


Figure 7. Energy-dispersive X-ray spectroscopy (EDS) spectrum of PZ96 Photocatalyst.

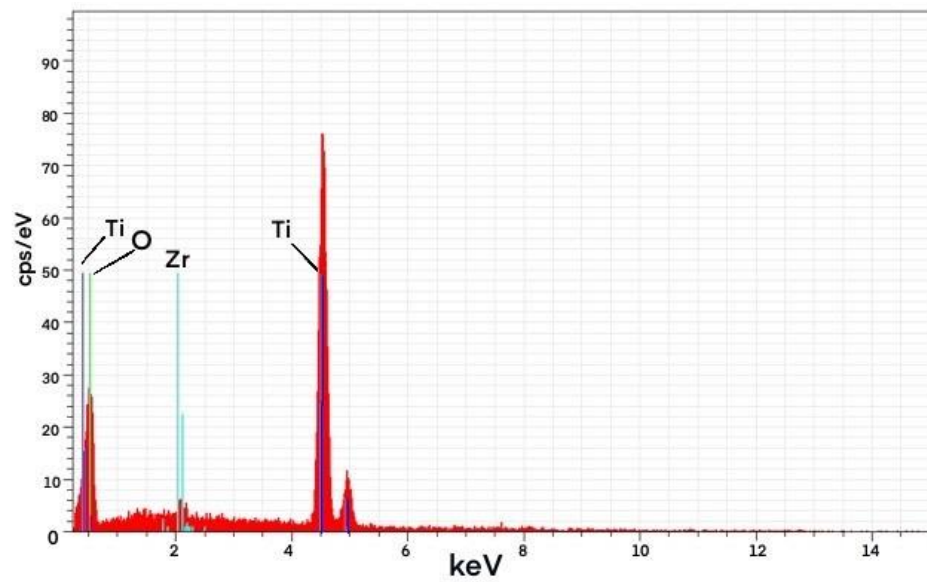


Figure 8. EDS spectrum of PZ192 Photocatalyst.

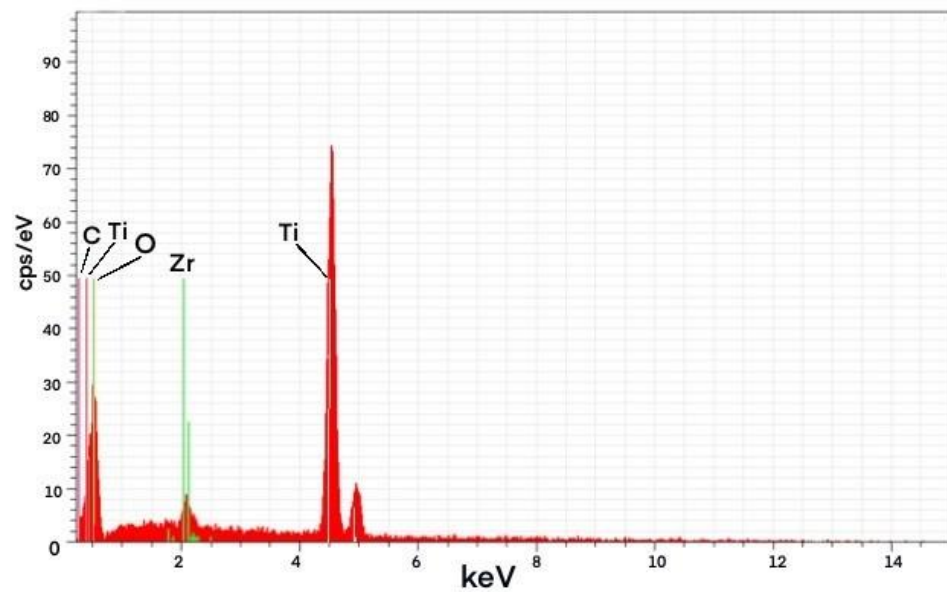


Figure 9. EDS spectrum of PZ480 Photocatalyst.

3.3. Analysis of P25/ZrO₂/GO

3.3.1. XRD Analysis of P25/ZrO₂/GO

When compared with JCPDS standard chart No. 21-1276, the diffraction peaks of P25 in P25/ZrO₂/GO were the same as the peaks of titanium dioxide (anatase), as shown in Figure 10. The peaks at $2\theta = 28.2^\circ$ and 31.4° are the characteristic peaks of a zirconium dioxide monoclinic crystal. The peaks at $2\theta = 35.2^\circ$, 50.6° , and 60.2° are the characteristic peaks of the zirconium dioxide cubic phase. Since the content of ZrO₂ we added was just a small amount, the peaks are not obvious. The peaks at $2\theta = 10.9^\circ$ and 43.53° are the characteristic peaks of graphene oxide, but the peaks are not clearly displayed due to small amounts of graphene oxide in P25/ZrO₂/GO.

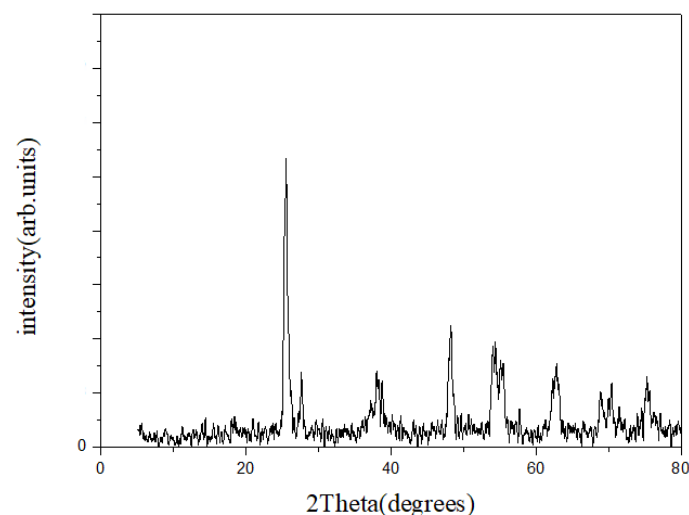


Figure 10. XRD analysis of P25/ZrO₂/GO.

3.3.2. Raman Analysis of P25/ZrO₂/GO

In the Raman analysis, as shown in Figure 11 and Table 5, the D band signal of graphene oxide was at 1357.5 cm^{-1} and the G band signal of was at 1595.9 cm^{-1} . The characteristic peaks of titanium dioxide (anatase) also appeared at 148 cm^{-1} , 398 cm^{-1} , 515 cm^{-1} , and 639 cm^{-1} . It was proved that P25 and graphene oxide were successfully compounded. After calculation, as the amount of graphene oxide increased, the ID/IG

ratio had a rising trend. This is because P25 was doped on graphene oxide, resulting in an increase in surface defects. This corroborates that documented in the literature [8].

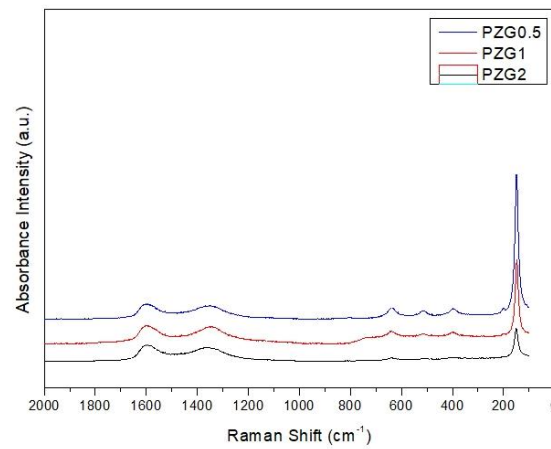


Figure 11. Raman analysis of PZG0.5, PZG1 and PZG2.

Table 5. I_D/I_G ratio of different ratios of P25/ZrO₂/GO.

	GO	PZG0.5	PZG1	PZG2
I_D/I_G	0.83	0.88	0.90	0.90

3.3.3. UV-Vis Analysis of P25/ZrO₂/GO

From Figure 12, when GO was added into the P25/ZrO₂, the initial absorption wavelength shows a redshift. The more the amount of graphene oxide added, the more the redshift occurs.

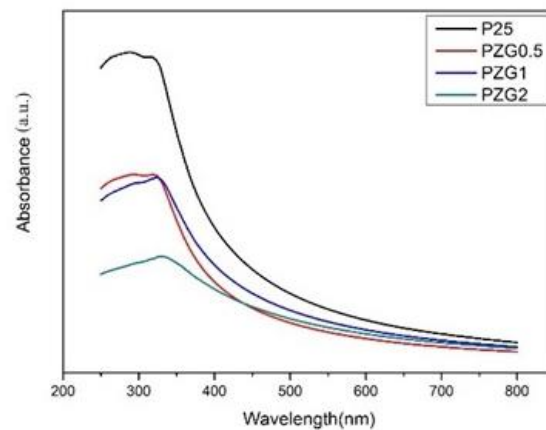


Figure 12. UV-Vis analysis of P25/ZrO₂/GO.

3.3.4. Energy Gap Analysis of P25/ZrO₂/GO

The absorption spectrum measured by UV-Vis spectrum was converted into Kubelka-Munk coordinates by the Kubelka-Munk function, and the energy gap of the material can be obtained as shown in Table 6 and Figure 13. After adding graphene oxide, the energy gap had a significant downward trend.

Table 6. Energy gap of P25/ZrO₂/GO.

	P25	PZG0.5	PZG1	PZG2
Energy gap	3.29	3.21	3.18	2.85

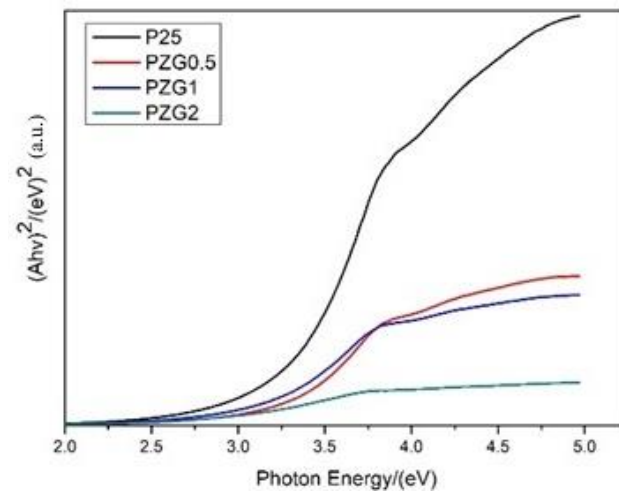


Figure 13. Energy gap analysis of P25/ZrO₂/GO.

3.3.5. SEM Analysis of P25/ZrO₂/GO

The field emission scanning electron microscope (FE-SEM) was employed to observe the surface morphology and agglomeration of the P25/ZrO₂/GO as shown in Figures 14–16.

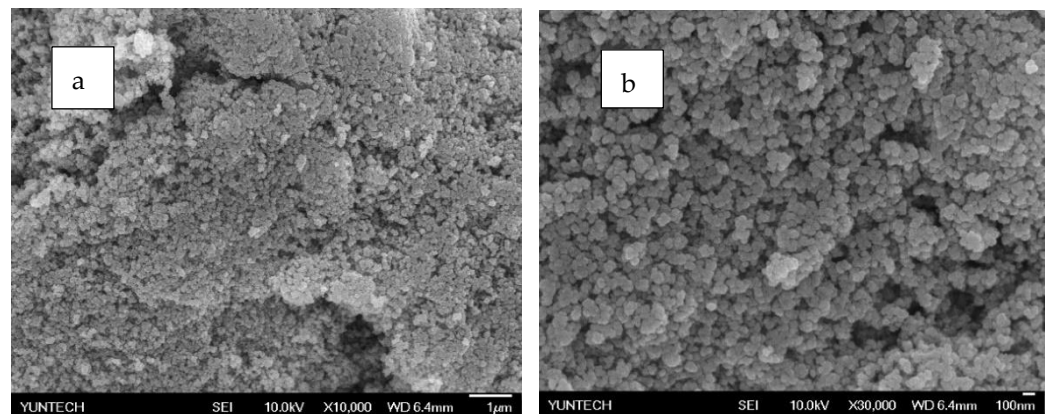


Figure 14. Scanning electron microscope (SEM) analysis of PZG0.5 (a) 10,000 times (b) 30,000 times.

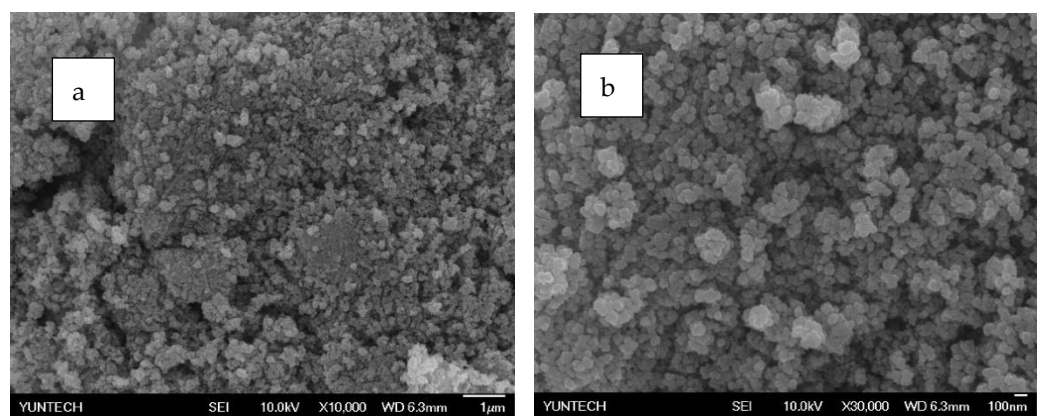


Figure 15. SEM analysis of PZG1 (a) 10,000 times (b) 30,000 times.

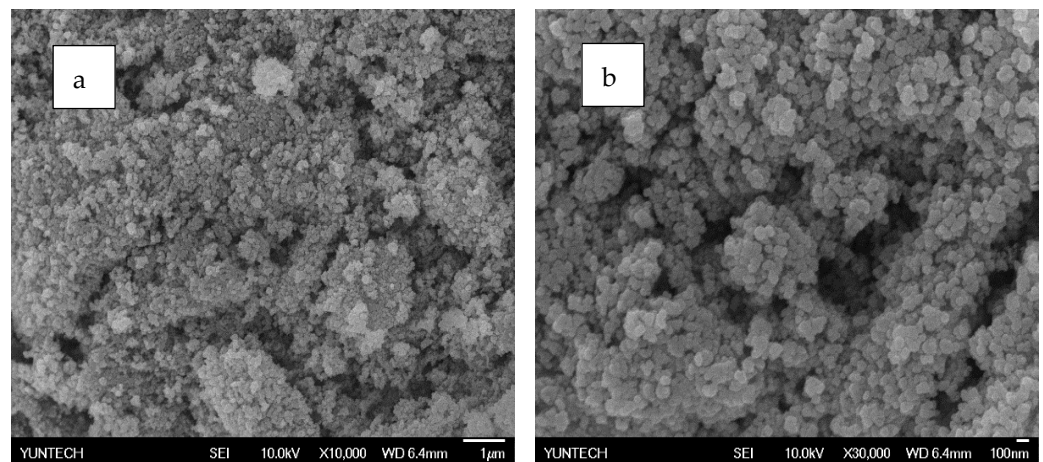


Figure 16. SEM analysis of PZG2 (a) 10,000 times (b) 30,000 times.

It can be seen from the SEM images that the more graphene oxide (GO) is added, the easier it produces agglomeration. This indicates that the agglomeration phenomenon of PZG2 was the most serious case.

3.3.6. SEM Analysis of P25/ZrO₂/GO Prepared by Electro spray Method

In Figures 17–19, the agglomeration of P25/ZrO₂/GO prepared by electro spray method could be reduced.

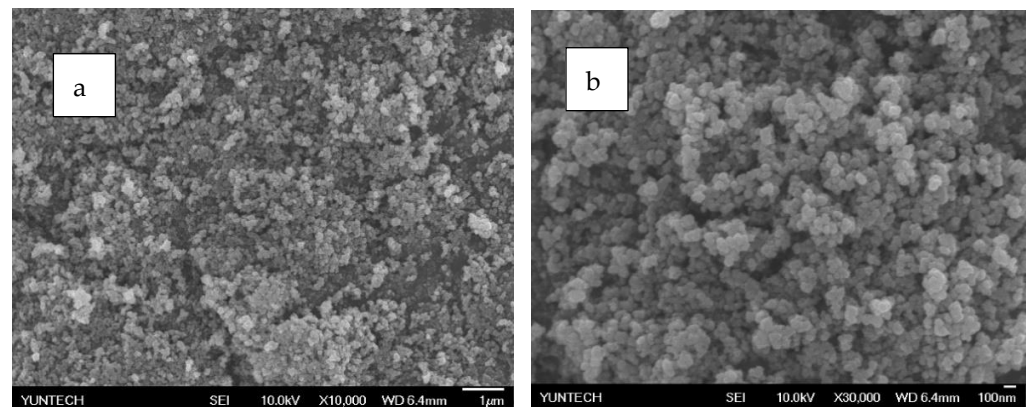


Figure 17. SEM analysis of PZG0.5 by electro spray method: (a) 10,000 times and (b) 30,000 times.

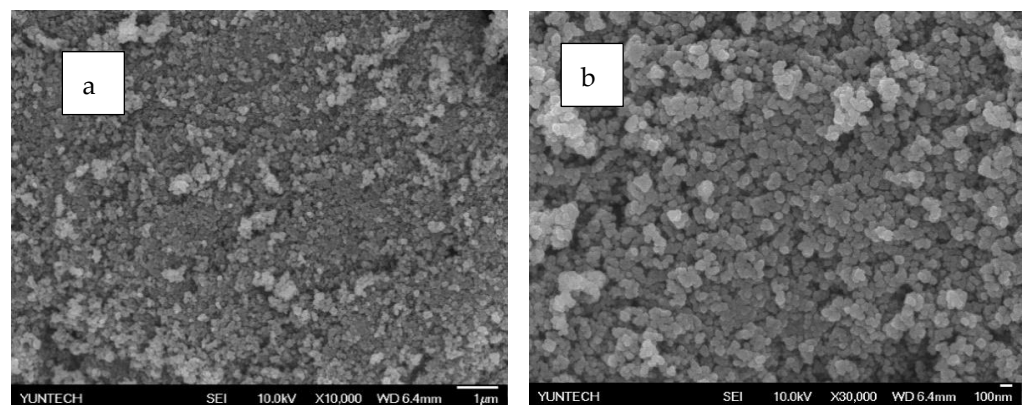


Figure 18. SEM analysis of PZG1 by electro spray method: (a) 10,000 times and (b) 30,000 times.

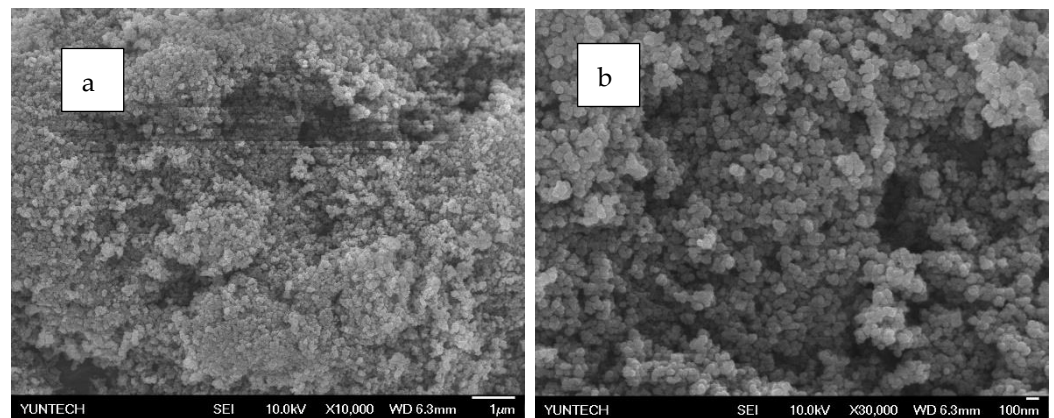


Figure 19. SEM analysis of PZG2 by electro spray method: (a) 10,000 times and (b) 30,000 times picture.

The applied voltage by the electro spray method could force the particles to separate leading to the decrease of agglomeration. However, the agglomeration could still be clearly seen in PZG2 by the electro spray method, because the content of graphene oxide (GO) is higher than that of the other two materials. Therefore, the agglomeration of graphene oxide (GO) and P25 is relatively high, and it is difficult to be alleviated after electro spray.

3.4. Photodegradation of Methylene Blue (MB)

3.4.1. Photodegradation Analysis of Different Ratios of P25/ZrO₂

The photodegradation rate of the P25 commercial photocatalyst was 42.63%. After adding zirconium dioxide, the photodegradation rate of the PZ96 photocatalyst was 46.38%, and the photodegradation rate of the PZ192 photocatalyst was 49.23%, as shown in Table 7 and Figure 20. The photodegradability had an upward trend. It can be proved that adding zirconium dioxide can help the photocatalyst attract electrons, reduce the probability of electron–hole recombination, and increase its photodegradation activity [9]. When 480 mg of zirconium dioxide was added, the photodegradation rate of the PZ480 photocatalyst decreased to 39.45%, which was lower than that of P25 commercial photocatalyst. There were two main causes of this. First, the energy gap of zirconium dioxide is about 5 eV. It is especially true that when too much zirconium dioxide is added, the quantum yield of the photocatalyst is reduced [10]. Secondly, adding too much zirconium dioxide may cover the photocatalyst surface excessively, and so this makes it unable to contact with the reactants, thereby resulting in a reduction in the photodegradation reaction [9]. These two factors lead to the decrease of photodegradation rate.

Table 7. Photodegradation of different ratios of P25/ZrO₂.

	Original Absorbance	Dark Absorption	Light Absorption	Photodegradation Rate	Solution Concentration
P25	3.58	3.24	1.72	42.63%	9.55
PZ96	3.58	3.27	1.55	46.38%	8.66
PZ192	3.58	3.19	1.39	49.23%	7.77
PZ480	3.58	3.19	1.74	39.45%	9.71

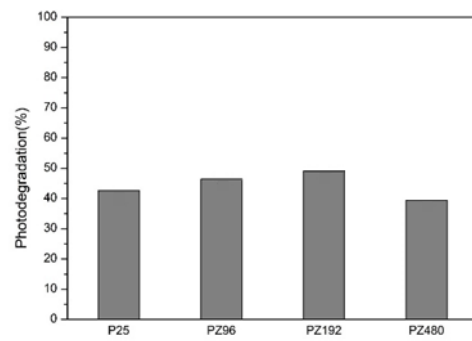


Figure 20. Photodegradation of different ratios of P25/ZrO₂.

3.4.2. Photodegradation of Different Ratios of P25/ZrO₂/GO

The photodegradation rate of PZG0.5 was 26.61%, the photodegradation rate of PZG1 was 38.35%, and the photodegradation rate of PZG2 was 17.47%, as shown in Table 8 and Figure 21. The photodegradation rates of the three were lower than that of PZ192, which had no content of graphene oxide. Due to the agglomeration of graphene oxide and P25 commercial photocatalyst [11], the particle size increased and the reaction surface area decreased, thereby resulting in a decrease in photodegradability. When graphene oxide was added up to 2%, the photodegradation rate of PZG2 was lower than those of the former two. When graphene oxide is added too much, it tends to produce a barrier on the surface. It becomes over-covered on the photocatalyst surface and is unable to contact with reactant, thereby reducing the photodegradation reaction [6,12].

Table 8. Photodegradation of different ratios of P25/ZrO₂/GO.

	Original Absorbance	Dark Absorption	Light Absorption	Photodegradation Rate	Solution Concentration
PZG0.5	3.58	2.68	1.66	26.61%	9.34
PZG1	3.58	2.60	1.19	38.35%	6.81
PZG2	3.58	1.56	0.99	17.47%	5.73

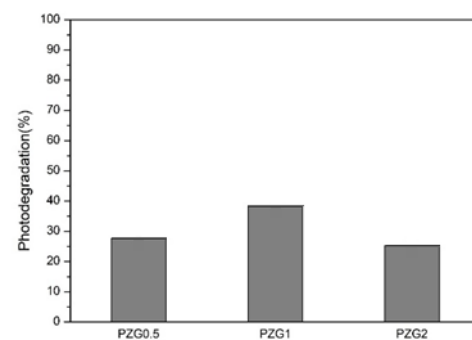


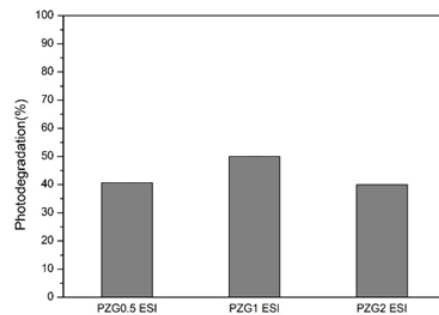
Figure 21. Photodegradation of different ratios of P25/ZrO₂/GO.

3.4.3. Photodegradation of Different Ratios of P25/ZrO₂/GO Made by Electrospray Method

The photodegradability of P25/ZrO₂/GO made by the electrospray method increased, as shown in Table 9 and Figure 22. The photodegradation rate of PZG0.5 ESI was 40.62%, the photodegradation rate of PZG1 ESI was 49.92%, and the photodegradation rate of PZG2 ESI was 39.92%. It proves that the electrospray method does reduce agglomeration [13], but it still fails to surpass the PZ192 in terms of photodegradability. Although the electrospray method can possibly reduce the agglomeration of particles, it cannot completely eliminate agglomeration.

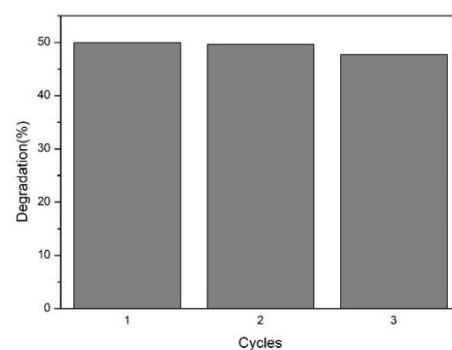
Table 9. Photodegradation of different ratios of P25/ZrO₂/GO made by the electro spray method.

	Original Absorbance	Dark Absorption	Light Absorption	Photodegradation Rate	Solution Concentration
PZG0.5 ESI	3.58	3.00	1.46	40.62%	8.28
PZG1 ESI	3.58	2.74	0.86	49.92%	5.02
PZG2 ESI	3.58	2.08	0.64	39.92%	3.84

**Figure 22.** Photodegradation of different ratios of P25/ZrO₂/GO made by the electro spray method.

3.4.4. Cyclic Photodegradation Test of P25/ZrO₂/GO1% Made by Electro spray Method

In order to test whether the PZG1 made by the electro spray method can be reused, methylene blue was degraded by the photocatalyst, and then washed with deionized water. The next degradation experiment was carried out under the same conditions. This involved three cyclic tests of photodegradation shown in Figure 23. In the first photodegradation test, the photodegradation rate was 49.92%. After washing the photocatalyst with deionized water, the second test was carried out, and the photodegradation rate was 49.65%. For the third test after ultrasonic washing, the photodegradation rate was 47.71%. The photodegradation rate indicates that the photocatalyst has good stability and reusability. In the cyclic test, the photodegradation rate gradually tended to decrease. This was mainly due to the quality of the photocatalyst losses caused by washing of the photocatalyst in the experiment [14].

**Figure 23.** Cyclic photodegradation test of P25/ZrO₂/GO1% (PZG1) made by the electro spray method.

3.5. Particle Sizes of P25/ZrO₂/GO Photocatalysts

The particle sizes of PZG0.5, PZG1, and PZG2 were 3396.0 nm, 3593.7 nm, and 6829.9 nm, respectively. The particle sizes of PZG0.5 ESI, PZG1 ESI, and PZG2 ESI were 373.8 nm, 516.9 nm, and 771.6 nm, respectively. The electro spray method can reduce the particle sizes.

4. Conclusions

ZrO₂/TiO₂ and ZrO₂/Graphene Oxide/TiO₂ was prepared successfully. After adding zirconium dioxide, the energy gap tended to decrease. After adding graphene oxide,

the energy gap had a significant downward trend. The photodegradation rate of the P25 commercial photocatalyst beside a Philips TL-D 8W/865 fluorescent tube for 4 h was 42.63%. After adding zirconium dioxide, the photodegradation rate of the PZ96 photocatalyst was 46.38%, and the photodegradation rate of the PZ192 photocatalyst was 49.23%. It can be proved that adding zirconium dioxide can help the photocatalyst attract electrons, reduce the probability of electron–hole recombination, and increase its photodegradation activity. The photodegradability of P25/ZrO₂/GO made by the electrospray method increases. The photodegradation rate of PZG1 ESI was 49.92%. We carried out three cyclic tests of photodegradation. In the first photodegradation test, the photodegradation rate was 49.92%. After washing the photocatalyst with deionized water, the second test was carried out, and the photodegradation rate was 49.65%. For the third test after ultrasonic washing, the photodegradation rate was 47.71%. The photodegradation rate shows that the photocatalyst has good stability and reusability.

Author Contributions: Conceptualization, Y.-H.N.; Investigation, J.-F.C.; Writing—original draft, C.-Y.F.; Writing—review & editing, M.-S.L. All authors have read and agreed to the published version of the manuscript.

Funding: This research received no external funding.

Conflicts of Interest: The authors declare no conflict of interest.

References

1. Hufschmidt, D.; Bahnemann, D.; Testa, J.J.; Emilio, C.A.; Litter, M.I. Enhancement of the photocatalytic activity of various TiO₂ materials by platinisation. *J. Photochem. Photobiol. A Chem.* **2002**, *148*, 223–231. [[CrossRef](#)]
2. Janus, M.; Inagaki, M.; Tryba, B.; Toyoda, M.; Morawski, A. Carbon-modified TiO₂ photocatalyst by ethanol carbonisation. *Appl. Catal. B Environ.* **2006**, *63*, 272–276. [[CrossRef](#)]
3. Lerf, A.; He, H.; Forster, M.; Klinowski, J. Structure of graphite oxide revisited. *J. Phys. Chem. B* **1998**, *102*, 4477–4482. [[CrossRef](#)]
4. Wang, S.; Sun, H.; Ang, H.-M.; Tadé, M. Adsorptive remediation of environmental pollutants using novel graphene-based nanomaterials. *Chem. Eng. J.* **2013**, *226*, 336–347. [[CrossRef](#)]
5. Jia, L.; Dong, L.; Zhu, L. Stripping voltammetry at graphene oxide: The negative effect of carbonaceous debris. *Appl. Mater. Today* **2017**, *8*, 26–30. [[CrossRef](#)]
6. Hamandi, M.; Berhault, G.; Guillard, C.; Kochkar, H. Reduced graphene oxide/TiO₂ nanotube composites for formic acid photodegradation. *Appl. Catal. B Environ.* **2017**, *209*, 203–213. [[CrossRef](#)]
7. Yang, W.-D.; Li, Y.-R.; Lee, Y.-C. Synthesis of r-GO/TiO₂ composites via the UV-assisted photocatalytic reduction of graphene oxide. *Appl. Surf. Sci.* **2016**, *380*, 249–256. [[CrossRef](#)]
8. Singh, I.; Kumar, R.; Birajdar, B.I. Zirconium doped TiO₂ nano-powder via halide free non-aqueous solvent controlled sol-gel route. *J. Environ. Chem. Eng.* **2017**, *5*, 2955–2963. [[CrossRef](#)]
9. Huang, C.; Ding, Y.; Chen, Y.; Li, P.; Zhu, S.; Shen, S. Highly efficient Zr doped-TiO₂/glass fiber photocatalyst and its performance in formaldehyde removal under visible light. *J. Environ. Sci.* **2017**, *60*, 61–69. [[CrossRef](#)] [[PubMed](#)]
10. Yikai, W. *Identification Analysis of TiO₂-ZrO₂ Photocatalyst Prepared by Sol-Gel Method and Study on Photocatalytic Kinetics of Decomposing Aldehydes*; Department of Chemical Engineering, Tsinghua University: Beijing, China, 2010; p. 6.
11. Tan, H.L.; Denny, F.; Hermawan, M.; Wong, R.J.; Amal, R.; Ng, Y.H. Reduced graphene oxide is not a universal promoter for photocatalytic activities of TiO₂. *J. Mater.* **2017**, *3*, 51–57.
12. Huang, X.; Wang, L.; Zhou, J.; Gao, N. Photocatalytic decomposition of bromate ion by the UV/P25-Graphene processes. *Water Res.* **2014**, *57*, 1–7. [[CrossRef](#)] [[PubMed](#)]
13. Jaworek, A.; Sobczyk, A.T. Electrospraying route to nanotechnology: An overview. *J. Electrostat.* **2008**, *66*, 197–219. [[CrossRef](#)]
14. Khodadadi, M.; Ehrampoush, M.; Ghaneian, M.; Allahresani, A.; Mahvi, A. Synthesis and characterizations of FeNi₃@SiO₂@TiO₂ nanocomposite and its application in photo-catalytic degradation of tetracycline in simulated wastewater. *J. Mol. Liq.* **2018**, *255*, 224–232. [[CrossRef](#)]